WILEY

Storage variability controls seasonal runoff generation in catchments at the threshold between energy and water limitation

Emilio Grande[1,2] 🄻 | Margaret A. Zimmer[1] 🄻 | John M. Mallard[3] 🄻

[1]Earth and Planetary Sciences Department, University of California Santa Cruz, Santa Cruz, California, USA

[2]Earth and Environmental Sciences Department, California State University East Bay, Hayward, California, USA

[3]Earth, Marine and Environmental Sciences Department, University of North Carolina Chapel Hill, Chapel Hill, North Carolina, USA

Correspondence
Emilio Grande, Earth and Environmental Sciences Department, California State University East Bay, Hayward, CA 94542, USA.
Email: emilio.grande@csueastbay.edu

Funding information
National Science Fundation, Grant/Award Number: EAR-1331846

Abstract

Annual water balance calculations may elide intra-annual variability in runoff generation, which could limit understanding of the similarities and differences between water- and energy-limited catchments. This may be especially important in comparisons between catchments close to the threshold between water- and energy-limitation. For this study, we examined runoff generation as a function of catchment storage in four watersheds, with focus on two that exist close to these thresholds, to identify how year-to-year variability in storage that results in intra-annual variations of runoff generation efficiency. Specifically, we focused on one energy-limited catchment in the humid subtropics and one water-limited catchment in a Mediterranean climate. We used measured and calculated daily water balance components to calculate variations in the relative magnitude of daily storage. We isolated precipitation events to draw connections between storage and runoff generation at intra-annual scales and compared our findings to the same metrics in two intensely energy-limited landscapes. We observed distinct stages in daily storage across water years in watersheds at the threshold, where systems experienced wet-up, plateau, and dry-down stages. During the wet-up, precipitation was partitioned to storage and runoff ratios (*RR*) were low. In the plateau, storage was filled and precipitation was partitioned to runoff, causing high *RR*s. During the dry-down, storage decreased as precipitation was partitioned to evapotranspiration and runoff, causing low *RR*s. The critical role of evapotranspiration during the growing season resulted in relatively higher *RR*s during the wet-up than during the dry-down for a given storage value. Thus, the same storage amount was partitioned to evapotranspiration or runoff differently throughout the year, depending on the storage stage. Despite their different positions on opposite sides of the threshold, the similarity between the two focus catchments suggests a potential characteristic behaviour of systems at the threshold common to both humid and semi-arid landscapes.

1 | INTRODUCTION

Precipitation partitioning between storage (*S*) and discharge (*Q*) is non-linear, dynamic and challenging to predict. The response characteristics of *Q* (i.e., runoff ratios [*RR*], magnitudes, recession rates)

remain notoriously challenging to predict (Spence, 2010; Davies & Beven, 2015). Even in the same catchment, varying *Q* responses to precipitation have been observed to depend on season or antecedent wetness conditions (Tromp-van Meerveld & McDonnell, 2006). The mechanisms mediating *Q* generation are often based on threshold-

controlled processes, produced by variability in S capacity at the hill-slope or catchment scale (Detty & McGuire, 2010), and are still incompletely understood.

Previous studies have focused on the hysteretic behaviour of S-Q relationships to describe catchment response to precipitation (P) events (e.g., [Davies & Beven, 2015; Hailegeorgis et al., 2016]). For example, characteristic curves of S-Q relationships have been used to describe periods of 'storing' (i.e., when dominant P partitioning processes cause the S increase to be much higher than the Q increase) and 'contributing' (i.e., when P is preferentially partitioned to Q instead of S) in an arid watershed in the sub-arctic Canadian shield (Spence et al., 2010). However, the dynamics of S at intra-annual time scales (e.g., aggregated precipitation events or monthly aggregates) remain poorly understood in many hydroclimates. As climate is often observed to serve as a first-order control on Q generation, (Spence et al., 2010) suggested that more catchment comparison work across different hydroclimates is needed to identify generalizable characteristics of S-Q relationships.

The hydroclimate of a watershed refers to the influence of climate on dominant hydrological and ecohydrological processes, and it can be described as the balance between water demand and supply. Commonly, P is used to describe water inputs and evapotranspiration (ET) to describe energy inputs. Energy-limited systems are characterized as systems where actual ET (AET) is approximately equal to potential ET (PET) because there is sufficient water supply to meet the PET demands. Water-limited systems are characterized as systems where AET is limited by water availability, so PET is not met. Event P partitioning across the spectrum of water-limited and energy-limited systems displays marked differences (Garcia & Tague, 2015; Jones et al., 2012). In wet, energy-limited systems, S may never go below threshold values needed for Q generation, and thus P can be consistently and preferentially partitioned directly to Q. Contrastingly, S is more likely to change in drier, water-limited systems during wet and dry periods. Therefore, in water-limited systems, it might be more evident that P's partitioning to Q might vary as a function of the S level of the system.

The water balance of a watershed, which describes differences in the water input, output, and S components, can be helpful for detangling hydroclimatic classifications. Water balance calculations are typically applied at time scales long enough (>1 year) that residual (S) can be assumed to be negligible. This helps facilitate catchment classification in terms of long-term hydroclimatic averages (e.g., in a Budyko, 1974 space for water- and energy-limited catchments) or to estimate one of its unknown components (often evapotranspiration, ET) from the other measured components (Rouholahnejad Freund & Kirchner, 2017). The wetness index, used in the Budyko (1974) space, which is described as the ratio of P relative to PET (Wagener et al., 2007), is a relatively simple method to visualize the hydroclimatic spectrum. However, differences or similarities regarding the mechanisms driving P partitioning to S or Q and the $S \sim Q$ relationships at intra-annual scales across watersheds on the hydroclimate spectrum are primarily unknown (Reaver et al., 2022).

Overarching hydroclimatic conditions might be a primary driver of event P partitioning characteristics, but interannual variability in total P may also play a critical role. Year-to-year variability in P may cause deviations of P partitioning from expected hydroclimatic behaviour. For example, (Nippgen et al., 2016) showed that P partitioning in a series of humid catchments in the Coweeta Hydrologic Laboratory in the southeastern United States varied between water-limited and energy-limited during dry and wet years, respectively. They also found that the annual P from the previous year was as significant as the current year's annual P for explaining the annual RR.

The intra-annual variability in P partitioning may not explain the differentiation between water- and energy-limited catchments, especially in catchments where the long-term hydroclimate characterizes them near the threshold between water- and energy-limitation ($P/PET = 1$). To address this knowledge gap, we used measured and calculated daily parameters of the water budget in energy-limited and water-limited catchments to identify event, monthly, and seasonal P partitioning behaviour. Notably, we sought to identify outlier events for which energy-limited watersheds behave like water-limited, or in which water-limited watersheds behave like energy-limited. Through this, we provide hypotheses for dominant and potentially universal controls on hydrologic partitioning through the lens of characteristic storage states. The present study extends over multiple water years and across four study catchments that span part of the hydroclimatic spectrum to understand differences and similarities in storage-driven hydrologic partitioning. Two catchments, one in the southeastern United States' humid subtropics (Calhoun Critical Zone Observatory [CZO]) and one in the semi-arid central coastal California (Tilden), fall on different sides of the water−/energy-limitation threshold, but experience year-to-year precipitation variability that causes these catchments to periodically switch between water- or energy-limited on an annual time scale. We compared results from these two catchments with two wetter, energy-limited catchments that do not switch designations, one maritime (Lower Hafren) and one tropical (Luquillo CZO). We used relative catchment storage to infer how other water balance parameters may control changes in Q processes at intra-annual timescales. Relative storage is an integrative variable of the water balance that incorporates current and antecedent hydrologic conditions. We chose this water balance-based approach to maximize comparability across catchments while also allowing us to identify opportunities for a more spatially distributed study.

2 | METHODS

2.1 | Research catchments

We primarily focused this study on two catchments located in humid and semi-arid climates. We compared the P partitioning from these catchments with two ancillary catchments from a maritime and a tropical climate, respectively.

The study system at Calhoun CZO is a 0.069 km^2 headwater catchment located in South Carolina, United States (U.S.; Figure 1).

FIGURE 1 Global map with the location of each study catchment starred. The hydroclimate classification is shown in colour (Peel et al., 2007). The climates legend only shows the four relevant climates for this study. Subset maps depict topography and catchment boundaries. Note the differences in scale between the catchments
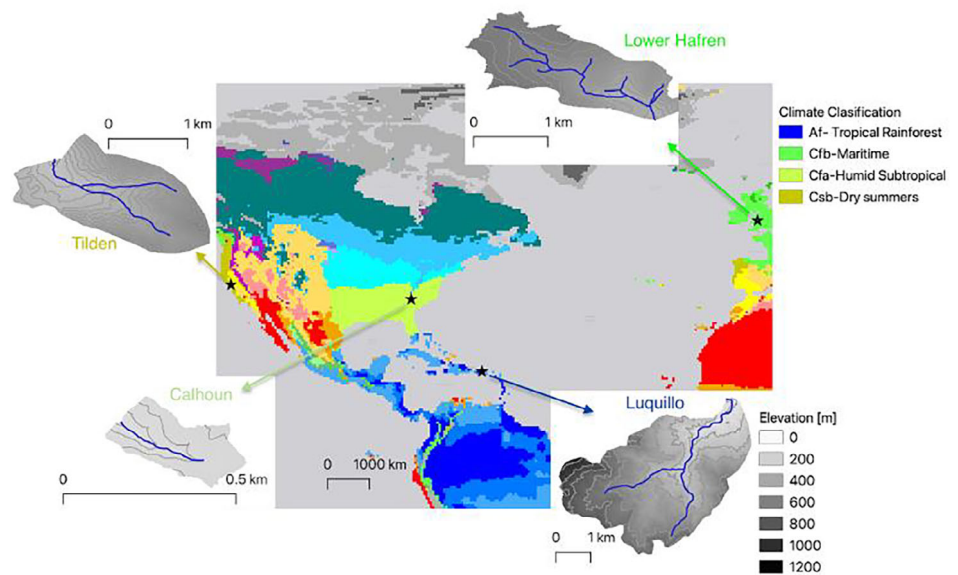
This area is part of the humid subtropical region of the Lower East Coast of the U.S. and is characterized by hot, humid summers and mild winters. Calhoun is located in an energy-limited hydroclimate, albeit near the threshold between water- and energy-limited conditions (Wlostowski et al., 2021). The catchment receives an average of 1200 ± 617 mm of P annually (1950–2015), evenly distributed across the year (~100 mm per month; Mallard, 2020). The mean annual ET is 800 ± 23.4 mm and the mean annual temperature is 16.3 ± 3.2°C (Mallard, 2020). The catchment has a total relief of 50 m, with elevations ranging from 124 to 173 m, and a median slope of 19% with a standard deviation of 13%. Soils are primarily Ultisols of the Appling, Cecil, and Madison soil series. These soils can be generally described as loamy sands overlying clay-rich argillic horizons, underlain by deeply weathered saprolite material (Richter et al., 2000). Soil depths generally increase moving away from the stream channel in Calhoun. Specifically, soil depths range from <1 m in or adjacent to stream channels to 4 m on narrow ridge tops to >9 m at Calhoun's upper divide, where it connects to a broader interfluve. The underlying geology is primarily granitic gneiss, the most common bedrock in the region. This headwater catchment is primarily forested in mixed hardwoods (e.g., *Carya spp.* and *Quercus spp.*) with minimal pine stands (*Pinus spp.*). Calhoun contains a non-perennial stream network that dries completely in the summer through early fall and flows primarily in late winter and early spring.

The Tilden watershed is a 3.4 km² headwater in Berkeley, California, U.S. (Figure 1) and is characterized by a Mediterranean water-limited hydroclimate, although near the threshold of water-energy limitation and can be energy-limited during extremely wet years. This system annually receives 930 ± 332 mm of P (2004–2018), with 80% of P occurring over the winter and spring months, a mean annual ET of 1030 ± 30 mm, and a mean annual temperature of 14.5 ± 7.6°C (Grande et al., 2020). Tilden has a total relief of 300 m, with elevations ranging from 282 to 580 m and a median slope of 16% with a standard deviation of 8.5%. The headwater is characterized by well-drained clay-loams and loam soils, formed in material weathered from mafic igneous rocks, varying in thickness from 0.3 to 1 m (Contra Costa Soil Survey, 1981). The area is underlain by a syncline, whose axis delineates the stream's course (Graymer, 2000) and likely controls the direction of groundwater flow (Grande et al., 2019). The Moraga Formation (Basalts from the Pliocene), which underlies the alluvium over much of the catchment, is of particular importance as a potential reservoir of groundwater. With a thickness of 10–25 m, it is considered one of the most important units for conducting groundwater flow in the study area (Zhou et al., 2003). Mixed forest covers approximately 48% of the watershed, evergreen forest covers 21%, shrubs and grasslands cover 20%, and the remaining 11% is covered by developed areas, including a golf course. A peculiarity of this catchment is the presence of a periodically irrigated golf course, which is an additional source of water considered in the water balance, albeit a minor one (Grande et al., 2020). A perennial stream drains the watershed.

Lower Hafren is a 3.5 km² experimental catchment in Wales, UK (Figure 1), where hydroclimatic data has been collected for decades. Lower Hafren is located in the cool-humid Cambrian Mountains. The catchment is energy-limited and receives a mean annual P of 2952 ± 426 mm (1993–2008), with a mean annual ET of 591 ± 56 mm and a mean annual temperature of 9.7 ± 8.3°C. Lower Hafren has a total relief of 310 m, with elevations varying from 670 to 360 m, with a median slope of 12% and a standard deviation of 15%. Stagnopodzols predominantly characterize Lower Hafren, but acidic peat, acid brown earth, and stagnogleys occur. Lower Palaeozoic slate, mudstone, greywacke, and sandstones compose the underlying geology (Harman, 2015). Lower Hafren is dominated by coniferous plantations (*Sitka Spruce* dominant). A perennial stream drains the watershed.

Luquillo is a 17.8 km² watershed part of the Luquillo CZO in Puerto Rico (Figure 1), where hydroclimatic data has been collected for decades. Luquillo is located in a tropical rainforest climate. This

watershed is energy-limited and receives a mean annual P of 3132 ± 1093 mm (Silver & Leon, 2019), the mean annual temperature is 24.2 ± 4.1°C, and the mean annual ET is 1305 ± 243 mm (Zimmerman, 2018). The catchment has a total relief of 760 m, with elevations varying from 4740 to 5500 m and a median slope of 28% with a standard deviation of 12%. Inceptisols and oxisols dominate the area, varying in thickness from 1 to 9 m, underlined by Cretaceous volcaniclastics (Buss et al., 2013). Luquillo is predominantly covered by Tabonuco, Palm, and Colorado forests. A perennial stream drains the Luquillo watershed.

Because all the watersheds used in this study are located in the northern hemisphere, hereafter, we use seasons for the northern hemisphere. Spring extends from March to May, Summer from June to August, Fall from September to November, and Winter from December to February. Further, the water year is considered to span from 1st October to 30th September, to encompass the rainy season for regions with strong seasonality in precipitation.

2.2 | Data description

We employed daily data collected by the authors from Calhoun and Tilden and publicly available hydroclimatic data from Lower Hafren and Luquillo. Data from Calhoun are limited to the 2015 water year (total P in the 35th percentile) and the 2016 water year (total P in the 79th percentile) and at Tilden to the 2017 water year (total P in the 100th percentile, the wettest year in the available record) and the 2018 water year (total P in the 40th percentile). Thus, we chose data from Lower Hafren (1992 water year and 2007 water year in the 40th and 92nd percentile, respectively) and Luquillo (2008 water year and 2010 water year in the 44th and 94th percentile, respectively) to capture similar precipitation percentiles across all four study catchments. Herein, we use 'Normal' and 'Wet' water years to refer to the water years in each catchment's lower and higher P percentile, respectively (Table 1).

The data from Calhoun were collected and maintained as described in (Mallard, 2020). Briefly, P was measured at the site with a tipping bucket rain gauge at a 0.1 mm/tip resolution. Q was calculated using stage measurements with redundant capacitance rods (TruTrack, ±1 mm) at five-minute intervals installed in the pool of a

90° v-notch weir built at the catchment outlet and was summed to daily. PET was determined from the Thornthwaite equation (Thornthwaite, 1948) using temperature data from the site as it has been shown that this method yields good estimates of AET for this site (Wlostowski et al., 2021). Further, we assumed that in energy-limited watersheds (e.g., Calhoun, Lower Hafren, and Luquillo), AET ≅ PET. We assumed that the monthly ET values obtained from the Thornthwaite equation were uniformly distributed within each day of the month to convert to daily ET.

Tilden's data was published in Grande et al. (2020). Briefly, P records were obtained from the open-access California Data Exchange Center (California Data Exchange Center–Query Tools, [CalETa, 2019]) operated by the California Department of Water Resources, which has an extensive hydrologic data collection network that includes P, with one station within the studied catchment. P was measured with a tipping bucket rain gauge, and data have been available for this location since February 2004. A particularity of this catchment is the presence of a periodically irrigated golf course (Grande et al., 2019, 2020). Because irrigation water is only applied in a small area of the watershed, and because this water is a small fraction compared to P (less than 3% over the 2-year period studied here), we combined the depth of irrigation water with P and considered them as a single component in the water budget. The stream stage was measured at an interval of 20 minutes with a pressure transducer (in-situ aqua troll multi-parameter meter Denver, Colorado, US), deployed in the same location since 2015 and maintained by the East Bay Regional Park District (EBRPD). Q was calculated from stage using a rating curve constructed by EBRPD staff. A correction factor was applied to flagged measurements of Q, as described in (Grande et al., 2020). ET data were provided by Formation Environmental LLC (CalETa), which developed, with support from the California Department of Water Resources, a data set for mapping daily AET through satellite observations (Paul et al., 2017).

The data used from Lower Hafren was previously used by (Harman, 2015), and over three decades of daily hydroclimatic data are available. P was measured at two weather stations within the watershed boundary and then averaged to obtain a single mean daily value. Q was calculated from stage measured in 90° v-notch weir installed at the watershed's outlet. PET was calculated from hourly automatic weather stations using the FAO Penman-Monteith

TABLE 1 Summary of annual water budget components by water year for each study catchment. RR is runoff ratio

Catchment	WY	WY type	P (mm)	P percentile	ET (mm)	Q (mm)	RR	ET/P
Lower Hafren	2007	Wet	3228	92nd	656	2659	0.82	0.20
Lower Hafren	1992	Normal	2651	40th	554	2001	0.75	0.20
Luquillo	2010	Wet	5331	94th	1311	3858	0.72	0.25
Luquillo	2008	Normal	3678	44th	1216	2825	0.77	0.33
Calhoun	2015	Normal	1159	35th	782	198	0.17	0.67
Calhoun	2016	Wet	1410	79th	775	554	0.39	0.55
Tilden	2017	Wet	2353	100th	1049	1054	0.45	0.45
Tilden	2018	Normal	994	40th	1005	310	0.31	1.01

equation (Allen et al., 1998). Further, Harman (2015) fitted a parameter k_E (1.63) to scale ET rates according to $ET = k_E PET$ and calibrated the long-term record to obtain AET (Kirchner, 2009). Hydroclimatic data from Luquillo is available through the Luquillo CZO database. P and Q datasets are available from Silver and Leon (2019), collected from stations managed by the U.S. Geological Survey and the U.S. Forest Service, and meteorological data are available from Zimmerman (2018). For Luquillo, we calculated PET from the Thornthwaite equation (Thornthwaite, 1948) using temperature data from Zimmerman (2018).

2.3 | Data analysis

2.3.1 | Catchment storage

Catchment storage was defined as an aggregated metric, combining various reservoirs (e.g., soil, regolith, bedrock). The daily catchment water budget was evaluated as:

$$\Delta S = P - Q - ET, \tag{1}$$

where ΔS is daily change in catchment S (mm/d), P is daily precipitation (mm/d), Q is daily runoff (mm/d), and ET is daily evapotranspiration (mm/d). Relative storage (mm) for each day (t) was estimated as:

$$S = \int_{t_0}^{t} (P - Q - ET)dt. \tag{2}$$

Relative S was calculated from the water fluxes described in the above sections for two water years at each study site, and Normal water year and a wet water year (Table 1). In Equation (2), t_0 is the first day of the water year (1st October), and $S_0 = 0$ at t_0. In the two watersheds at the threshold of water-energy limitation, October 1st corresponds to the driest part of the year. Thus, we assumed that S was at a minimum at the start of the water year. We conceptualized S as a lumped metric, aggregating numerous reservoirs (e.g., soils, alluvial deposits and regolith). We calculated antecedent S as the value of S on the first day of a P event. Further, we examined the relative water balance for individual P events (Section 2.3.2), and relative S (mm/d) was recalculated for each event, starting at a relative value of zero ($S_0 = 0$).

2.3.2 | Precipitation event delineation and characterization

Hydrologic partitioning studies are often conducted over individual precipitation events. However, delineating precipitation events is not consistent throughout the scientific literature. Precipitation events may refer to specific periods during which P falls in a catchment. For example, (Singh et al., 2018) classified precipitation events as periods with at least 30 min of rainfall with total rainfall greater than 20 mm,

and events were separated by at least 3 h with no rainfall. (Rinderer et al., 2016) defined precipitation events based on a P threshold of 5 mm, the average P for days when rainfall occurred, and events were separated by at least 2 h without measured P.

Rainfall events have also been delineated from the hydrograph times series. Some studies have used a threshold value of Q (Rose & Peters, 2001), a percentage threshold in response to groundwater height change (Meerveld et al., 2015), and baseflow separation to delineate events (Blume et al., 2007; Merz et al., 2006). (Detty & McGuire, 2010) used an inclusive approach where they defined events as the interval from the start of P to the end of quickflow, defined as the portion of the hydrograph composed of stormflow contributions from rapid surface runoff or interflow. (McCarter et al., 2020) used a similar approach where they selected precipitation events from the onset of P to the time when Q had receded to near or pre-event conditions, and changes in Q were <0.1 mm/day for two consecutive days. Lastly, studies such as that of (McGlynn & McDonnell, 2003a, 2003b) zoomed in on a single or a few events with no rigorous definition stated.

Here, we defined precipitation events from the onset of $P \geq 1$ mm/day to when Q had receded to 120% of pre-event conditions or when another event started (marked by a positive slope in the hydrograph) before Q receded back to the 120% threshold. Considering that the precipitation regimes vary across the studied catchments, and since our approach requires us to extract periods across the entire water year for comparison, we used this inclusive approach of using both P and Q to delineate precipitation events. We identified 301 events across the study period, with 89, 54, 84, and 74 events from Calhoun, Tilden, Luquillo, and Lower Hafren, respectively (shaded regions in Figure 2).

We calculated the RR by dividing event flow by total rainfall. We calculated event-flow using a baseflow separation algorithm based on recession analysis (Sujono et al., 2004) in the EcoHydRology R package (Fuka et al., 2018). Due to their simplicity, hydrograph recessions are widely used in watershed hydrology (Smakhtin, 2001). This methodology has been successfully used on daily streamflow time series (Choi et al., 2022; Kottegoda et al., 2000; Santos et al., 2018), and thus it was preferred in our analysis. For analyses comparing precipitation events of different lengths and across different sites, we normalized total event P (Q or ET) by the length of the event, hereafter referred to as normalized event values.

3 | RESULTS

3.1 | Annual hydrologic budget

The normal water year at Calhoun totaled 1159 mm of P, representing ~41 mm less than the mean annual P (Figure 2). ET and Q removed 782 and 198 mm during the normal water year, respectively. The annual RR during the Normal water year was 0.17 and ET/P was 0.67 (Table 1). The wet water year began with Hurricane Joaquin in late September 2015 (NOAA, 2015), bringing approximately
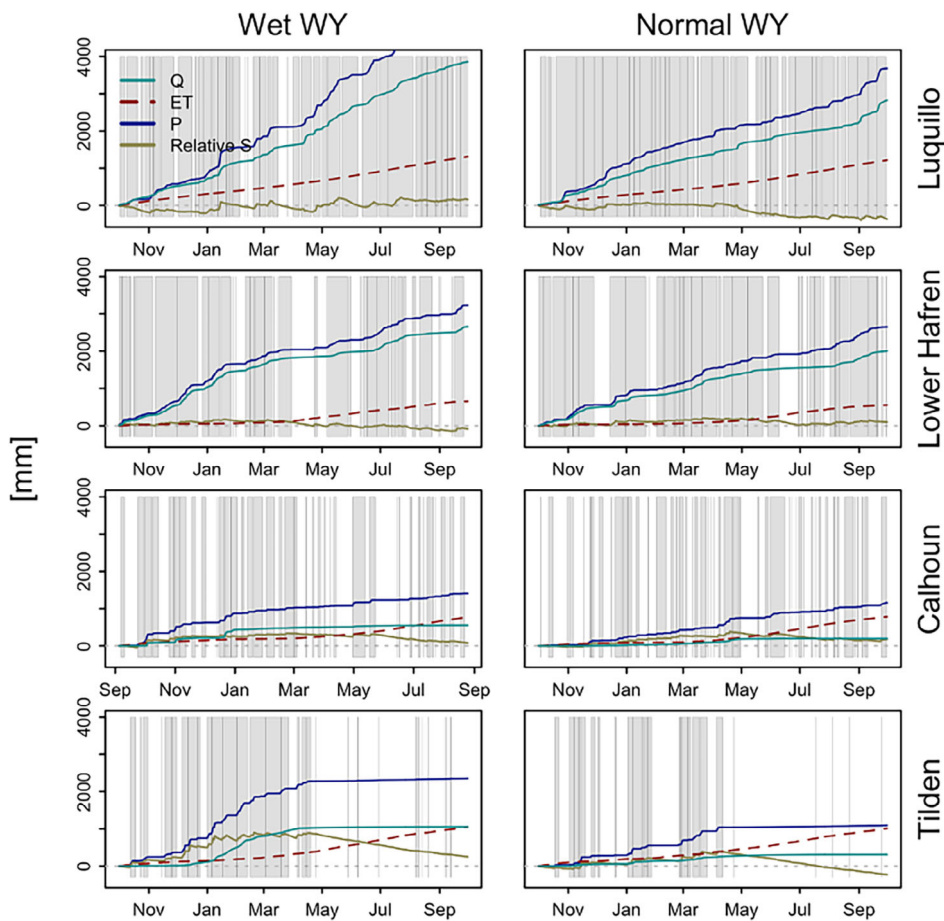
FIGURE 2 Cumulative daily values of precipitation (*P*; blue line), evapotranspiration (*ET*; green), runoff (*Q*; teal), and relative storage (*S*; red) over two full water years for the four study catchments. The shaded regions mark each of the 301 precipitation events analysed in this study

300 mm of rainfall over 1 week, representing 20% of the total *P* in the water year (1410 mm, Figure 2). This resulted in a "wetter" water year with a higher *Q* of 554 mm and a corresponding higher *RR* than the normal water year (0.39). In contrast, *ET* was 775 mm, only 7 mm lower than the previous, somewhat drier water year. During the wet water year, *ET/P* was 0.55.

The normal water year at Tilden received 994 mm of *P*, 64 mm higher than the mean annual value for the catchment. Annual *ET* for the normal water year was 1005 mm, annual *Q* was 310 mm, the annual *RR* was 0.31, and *ET/P* was 1.01 (Table 1). The wet water year at Tilden was one of the wettest water year on record, with a total *P* of 2353 mm, doubling the 14-year annual average for the area (Figure 2). *ET* removed 782 mm of water from the catchment during this period, the annual *RR* was 0.45, and *ET/P* was 0.45. *Q* was three times higher in the wet water years than in the normal water years. Moreover, we found a shift between water-limited in the normal water year and energy-limited in the wet water year at Tilden (Table 1).

Lower Hafren is characterized by a relatively high annual *RR* (∼0.8), with *ET* removing 605 ± 72 mm (∼20% of *P*) for the two water years. Similarly, Luquillo is characterized by a relatively high *RR* of ∼0.75 for the two studied water years, and *ET* was responsible for removing 1264 ± 67 mm (∼25% of the *P*) over the studied period.

Catchments across the hydroclimatic spectrum studied here show that *P* is spatiotemporally variable, ranging from 994 mm/y in the normal water year at Tilden to 3228 mm/y in the wet water year at Luquillo. However, water outputs, particularly *ET*, are not as highly variable, ranging between 591 mm/year during the normal water year at Lower Hafren and 1311 mm/year in the wet water year at Luquillo. This discrepancy between the variability in water and energy inputs is reflected in the runoff variability, where catchments that receive more *P* have more extensive *Q* (e.g., Lower Hafren, Luquillo). Furthermore, *ET/P* is highly variable across sites, ranging from 0.2 at Lower Hafren to 1.01 at Tilden (Table 1), driven by *P* variability (Figure 2).

Although *P* is only 250 mm higher (∼1.2 times higher) in the wet water year at Calhoun than in the normal water year (1410 mm and 1159 mm, respectively), *Q* is 2.8 times higher. This indicates that the somewhat slight increase in *P* caused a substantial increase in *Q*. At Tilden, *Q* was 3.4 times higher in the wet water year than in the normal water year, but annual *P* was 2.3 times higher, suggesting that a significantly higher *P* is needed to achieve higher *RR*s at Tilden (Table 1). The catchments on the far end of the energy-limited spectrum (i.e., Luquillo and Lower Hafren) displayed somewhat negligible differences in the water budget components from year to year.

There is considerable contrast in *P* event frequency between Tilden and the other three catchments. While *P* was somewhat equally distributed over the water year at the other sites, *P* was restricted to

FIGURE 3 Relative catchment storage (line) delineated by the different storage stages (colour boxes). Light blue demarcates the wet-up stage, dark blue represents the plateau stage, and the wet down stage is marked by the red colour. The bars illustrate monthly runoff ratios (secondary vertical axis). The black points show event runoff ratios. All runoff ratios were calculated as event flow over total rainfall. The monthly runoff ratios are calculated as the total runoff for a given month (after baseflow separation) divided by total rainfall for the month
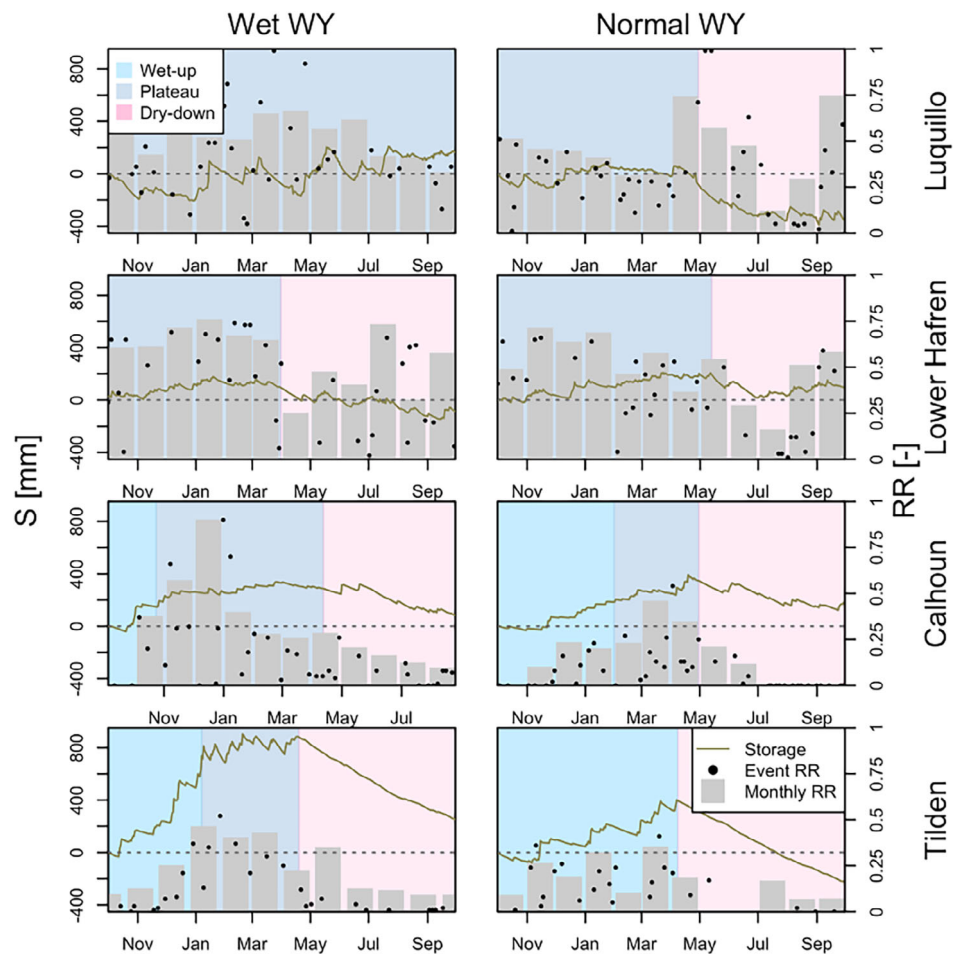
late fall and early spring at Tilden, with 94 ± 6% of *P* occurring between October and April. On the other hand, *ET* is seasonal in all catchments, with a marked increase in April or May. The *ET* seasonality is somewhat less pronounced in Luquillo, where high temperatures year-round and dense vegetation remove water from the catchment uniformly throughout the water year.

3.2 | Seasonal changes in precipitation partitioning

For the selected events in the wet water year in Calhoun (2015), *P* was 0.6 to 28.5 mm/d in summer and fall respectively (median = 6.6 mm/d). Event *ET* varied between 0.2 and 4.6 mm/d in winter and summer, respectively (mean = 2.3 mm/d). Event *Q* ranged between 0 (i.e., no flow or below detection limit) and 19.4 mm/d in summer and winter, respectively (mean = 1.7 mm/d). Event *RR* was 0 to 0.9 for summer and winter, respectively (mean = 0.2).

For the selected events in the normal water year at Calhoun (2016), event *P* varied between 0.4 and 20.7 mm/d in spring summer and spring, respectively (mean = 0.4 mm/d). Event *ET* was 0.2 to 4.4 mm/d in winter and summer, respectively (mean = 2.2 mm/d). Event *Q* was 0 to 4.7 mm/d in summer and spring, respectively

(mean = 0.5 mm/d). Event *RR* varied between 0 and 1 in summer and winter, respectively (mean = 0.1). In both water years from Calhoun, the event *RR*s increased from the onset of the water year and then decreased in mid-to-late spring (Figure 3).

At Calhoun, *P* partitioning to *S* varied between 0 (no *P* was partitioned towards storage) and 97%. These variations in *P* partitioning were seasonal, with the largest partitioning to *S* at the beginning of the water year (e.g., Figure 4a) and the largest partitioning towards *Q* occurring in the winter and spring (e.g., Figure 4b). A predominant partitioning of *P* to *ET* was observed for events in mid and late summer (e.g., Figure 4C).

During the wet water year at Tilden (2018), event *P* varied between 1.1 and 35.3 mm/d in summer and winter, respectively (mean = 10.7 mm/d). Event *ET* was 0.3 to 4.8 mm/d, in winter and summer, respectively (mean = 1.8 mm./day). Event *Q* was 0 to 10.2 mm/d, in summer and winter, respectively (mean = 1.8 mm/d). Event *RR* was 0 to 0.52 (mean = 0.1), with the higher values in winter.

During the normal water year (2017), event *P* was 0.3 to 25 mm/d in late spring and summer, respectively (mean = 8.4 mm). Event *ET* was 0.5 to 5.4 mm/d in winter and summer, respectively (mean = 2 mm/d). Event *Q* ranged between 0 and 3.3 mm/d in summer and spring, respectively (mean = 1.3 mm/d). Event *RR* was 0 to
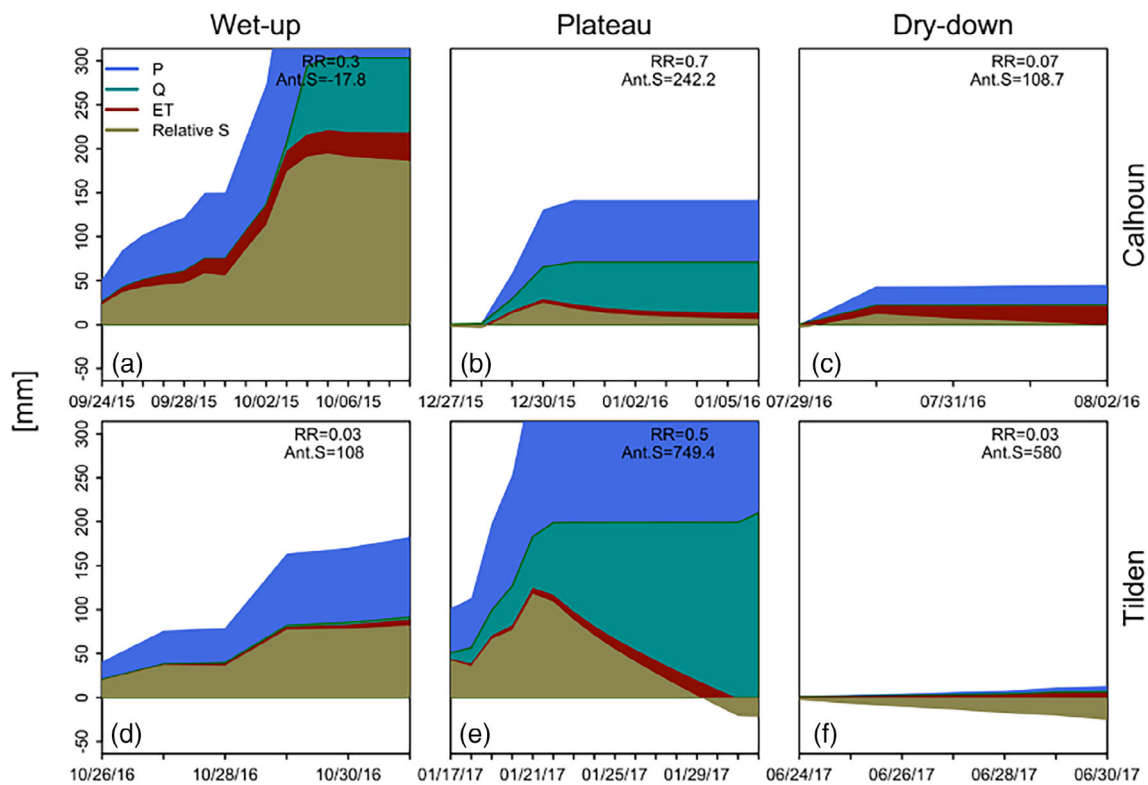
FIGURE 4 Specific precipitation events across the three catchment storage stages (wet-up, plateau, dry-down), illustrating changes in the relationship between storage and runoff. In the wet-up period, *S* increases and *RR*s are low. During the plateau, storage stays relatively constant while runoff is generated. During the dry-down, *S* and *RR* decrease. S is zero-ed out at the beginning of each event and integrated over the length of the event. The value of relative storage (*S*) for the water year on the first day of the event is listed as ant. *S* (antecedent storage) in the upper right-hand corner of each plot

0.41 (mean = 0.14). Like in Calhoun, the event *RR*s tended to increase as the water year progressed and decreased in spring, with the onset of the growing season (Figure 3).

Like in Calhoun, *P* partitioning was seasonal at Tilden. Early in the water year, *P* was partitioned preferentially towards *S* (e.g., Figure 4D), and predominant *Q* partitioning was observed in winter and early spring (e.g., Figure 4e). In Tilden, *P* partitioning to *S* varied between 0 and 90%. The somewhat smaller events in Tilden during the summer indicated that *P* is partitioned to *S* but because *ET* is high during this time, it depletes *S* back down (e.g., Figure 4f).

At Lower Hafren, event *P* was 1.25 to 25.3 mm/d (Table 2), with the most substantial events occurring in late fall and winter, with large events still occurring in summer. Event *ET* varied from 0.3 to 5.4 mm/d in winter and summer, respectively. Event *Q* ranged between 0.7 and 25.4 mm/d in summer and late fall. Event *RR*s were relatively high, with a mean of 0.4 across all seasons.

In Luquillo, the largest event accumulated 45.5 mm/d of *P* during summer, and the smallest event accumulated 0.2 mm/d in the fall. During the two water years analysed, event *ET* varied between 4.5 and 2.29 mm/d in summer and winter, respectively. Event *Q* ranged between 27.7 mm/d and 2.7 mm/d in spring and late fall respectively. The event *RR*s were relatively high, with a mean value of 0.4.

3.3 | Hysteresis in the storage dependency of runoff generation

In the catchments at the water−/energy-limitation threshold, we observed low *RR* and antecedent *S* values at the start of each water year. Relatively higher *RR* occurred at higher values of antecedent *S* as the water year progressed into the dormant winter (Figure 3). However, antecedent *S* and *RR* declined during the growing season as *ET* became a more prominent water balance component. This decline occurred in watersheds across all the studied hydroclimates, except for Luquillo in the wet water year. Based on this common pattern in S across water years and sites, we categorized *S* seasonality into three different stages: wet-up, plateau, and dry-down (Figure 3).

Catchments on either side of the water- and energy-limited threshold display different *S-RR* relationships (Figure 5), and even catchments at the threshold exhibit different behaviour. In the catchments near the water−/energy-limited threshold (Tilden and Calhoun), the *S-RR* relationship revealed hysteretic behaviour with a clockwise direction across each water year (Figures 3 and 5b,d). The water-limited catchment (Tilden) displayed large variability in antecedent *S* and a relatively small range of *RR*, which drove the hysteretic loop into a wide clockwise loop. Calhoun, the energy-limited catchment, showed greater variability in *RR* compared to Tilden and a

TABLE 2 Summary statistics of the precipitation events analysed in this study. SD refers to the standard deviation. Note that the values for event P, ET and Q values are statistics of the normalized values

	Calhoun	Tilden	Lower Hafren	Luquillo
Max P (mm/d)	28.5	35.3	25.3	45.5
Min P (mm/d)	0.4	0.84	1.25	0.2
Mean P (mm/d)	6.3	10	9.4	12.1
Median P (mm/d)	5.2	7.3	7.8	8.3
SD P (mm/d)	5.3	8.9	5.4	10.1
Max Q (mm/d)	19.7	16.9	21.4	27.7
Min Q (mm/d)	0.0	0.0	0.7	2.7
Mean Q (mm/d)	1.2	2.4	6.1	8.4
Median Q (mm/d)	0.4	1.0	4.8	7
SD Q (mm/d)	2.8	3.5	4.6	5.4
Max ET (mm/d)	4.6	5.4	4.4	4.5
Min ET (mm/d)	0.2	0.3	0.2	2.29
Mean ET (mm/d)	2.2	1.9	1.4	3.4
Median ET (mm/d)	1.7	1.7	1.1	3.3
SD ET (mm/d)	1.5	1.2	1.0	0.7
Max RR (−)	1	0.5	1	1
Min RR (−)	0	0	0.01	0.01
Mean RR (−)	0.1	0.1	0.4	0.4
Median RR (−)	0.1	0.1	0.4	0.3
SD RR (−)	0.2	0.1	0.25	0.25
Max length (d)	16	17	24	27
Min length (d)	1	1	1	1
Mean length (d)	4	5.1	6	8.1
Median length (d)	3	4.5	6.3	7
SD length (d)	3	4.2	6	4.8
n	89	54	74	84

relatively small range of antecedent S, causing a narrower and taller hysteretic loop (Figure 5). In contrast, hysteretic behaviour was not observed in the S-RR relationship for the strongly energy-limited watersheds (i.e., Luquillo and Lower Hafren; Figures 3 and 5a,c). In these systems, P appeared to be frequent enough to maintain an elevated catchment S, thus S was not as variable in Luquillo and Lower Hafren as in catchments near the threshold. This process leads to flashier streams in these strongly energy-limited catchments, explaining their more linear runoff response to precipitation events (Figure 2).

watersheds across the hydroclimatic spectrum, further limiting our ability to identify generalizable hydrologic processes. Here, we analysed event, seasonal and annual water balances across four catchments to address this knowledge gap. Specifically, we chose catchments we expected to have the highest dependence on storage for runoff generation, such as catchments near the threshold between water and energy limitation, with seasonal, highly variable runoff. Below, we use these results to generate hypotheses for dominant controls on catchment S and P partitioning that can be investigated in future studies.

4 | DISCUSSION

While watershed hydrology and hydroclimatology research efforts in recent decades have advanced our understanding of P partitioning to S or Q, we have limited approaches that can generalize and quantify P partitioning mechanisms affected by intra-annual variations in hydroclimatic properties (e.g., temperature, precipitation). Further, we have limited comparisons of S-Q relationships at intra-annual scales in

4.1 | Catchment storage drives runoff generation

Across the hydroclimatic spectrum considered in our study, event RRs exhibited a strong relationship with S (Figure 3). We used the RR metric to describe watershed runoff generation efficiency and observed that S adequately represents the underlying internal catchment functioning that drives runoff generation mechanisms (Hewlett & Hibbert, 1967). We can see the central effects of S on runoff
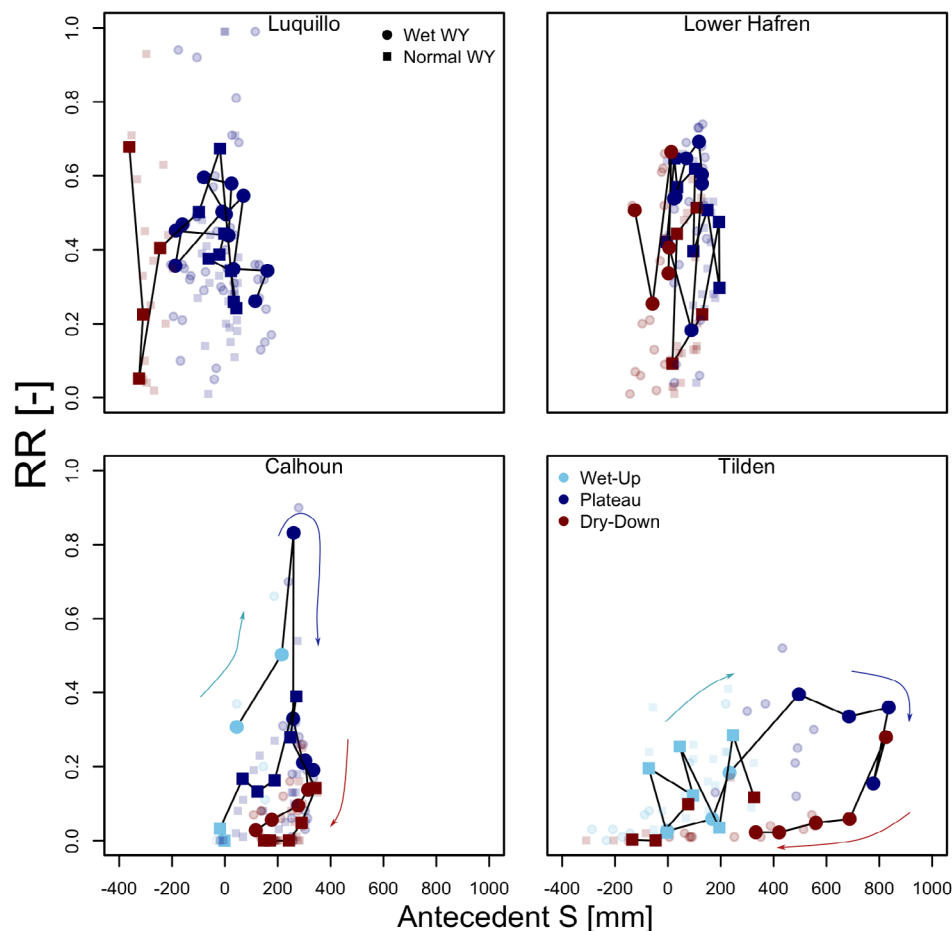
FIGURE 5 Runoff ratio (*RR*) versus antecedent storage across the four studied watersheds. The colours indicate the different stages of catchment storage (light blue, blue, and red indicate wet-up, plateau, and dry-down, respectively). The shape of the symbol indicates the type of water year (square and circle for normal and wet water years, respectively). The larger, opaque symbols represent monthly data while the smaller, transparent symbols correspond to individual events. The arrows in the Calhoun and Tilden plots highlight the clockwise hysteresis observed in these landscapes

generation for the catchments considered in this study as higher S results in higher RR (Figure 4). It is worth noting that the close relationship between S and RR in our study sites results from the runoff generation mechanisms that likely dominate at our sites, such as saturated subsurface flow and saturated overland flow (Lapides et al., 2022). Therefore, our findings should be generalized to catchments where the same assumed or known dominant runoff generation processes are similar to our sites. In catchments dominated by Hortonian Overland Flow and high-intensity rainfall events, with high-intensity rainfall and low infiltration where Hortonian overland flow dominates (largely arid or urban systems), increasing S would not necessarily lead to increasing RRs (van De Giesen et al., 2000; Woolhiser et al., 1996).

Intra-annual changes in S represent a kind of 'watershed memory' (i.e., the influence of past P inputs) in seasonal runoff generation patterns (Aulenbach & Peters, 2018). Previous studies have used other proxies for storage, such as antecedent precipitation indices, or water table measurements. However, here we use a direct estimation of storage. The tradeoff is likely in uncertainty. Water balance is a direct estimation of integrated storage, but it is likely uncertain. Further, researchers have explored event or monthly scale relationships between RRs and S and illuminated the significance of intra-annual S variability for runoff generation. For example, Nippgen et al. (2016) analysed the lag correlation among monthly P and RRs in five watersheds in the southeastern US and determined that monthly RRs were

most significantly correlated with the previous month's P and stayed strongly correlated up to a lag of 6 months. Others have explored P partitioning as a function of seasonality and catchment characteristics using theoretically derived and physically-based water balance models, suggesting that RR decreased with a decreasing wetness index (Yokoo et al., 2008). Yokoo et al. (2008) also suggested that the consequences of seasonality are most significant when the seasonal variabilities of P and ET are out of phase, such as in Mediterranean climates (e.g., Tilden) and in arid systems. Other modelling approaches have used precipitation partitioning at monthly scales based on the Budyko framework (Wang et al., 2011). Wang et al. (2011) showed that analysing the water balance at monthly scales, accounting for S variability, has the potential for understanding monthly, seasonal, and annual runoff generation. The work presented in the literature and our results highlight the role of watershed S in moderating P partitioning at intra-annual timescales that resulted in different runoff responses across the studied water years (Figure 3). Furthermore, our findings seem to be transferable across several regions in the hydroclimatic spectrum (Figure 3).

4.2 | Conceptual model of how dominant catchment states drive precipitation partitioning

Here, we present a conceptual model that characterizes differences and similarities in storage-driven hydrologic partitioning, informed by
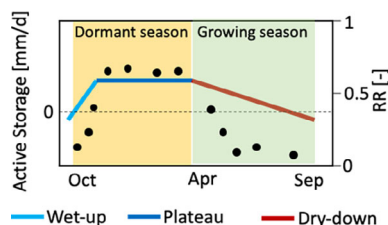
FIGURE 6 Conceptual model of stages of catchment storage. Runoff ratios are shown to be higher during the plateau, after storage is 'full.' note that the timing of the dormant and growing season is for the eastern US. The black dots represent runoff ratios

observations of P partitioning in four catchments that span part of the hydroclimatic spectrum of water- to energy-limitation. We summarized the seasonality in S over a water year, focusing on catchments near the threshold of water/energy-limited hydroclimates, where storage is depleted and recharged each water year (Figure 6). Based on daily water balance observations and the general shape of catchment storage, we divided S into three dominant stages across a given water year: wet-up, plateau, and dry-down. From the three S stages, we identified the wet-up and the dry-down as transitional stages towards or from the plateau, respectively (Figure 3).

4.2.1 | Wet-up

The onset of the wet-up stage occurs at the beginning of the water year when S is at a minimum and continues until S fills up. Because S starts low, P is mostly partitioned towards S (Tromp-van Meerveld & McDonnell, 2006; Zehe et al., 2005). That is, S 'fills up' during this wet-up, and minimum contributions to Q are observed (Figures 3 and 4). Because most of the wet-up stage coincides with the dormant season, ET is relatively low (Evers et al., 2021; Hay & Irmak, 2009) and changes to catchment S are predominantly influenced by P inputs and Q outputs.

4.2.2 | Plateau

Once S peaks, we transition to the plateau stage in the wet dormant season (Figure 6). During the plateau, we observe that P is predominantly partitioned to Q because, at this point, S capacity has likely been reached (Camporese et al., 2019). This is analogous to a full bucket (Dralle et al., 2018), which represents saturation of catchment S, and creates the conditions for the most dynamic period of runoff generation, with faster and higher magnitude stream responses to P inputs, as evidenced by relatively larger RRs (Figure 3). The runoff responses during the plateau suggest hydrological connectivity that favours water transfer as Q towards the catchment outlet (Soulsby et al., 2015).

The plateau stage contrasts with the beginning and end of the wet-up and dry-down, respectively, where S is low. The plateau stage

is likely more common or sustained for longer in energy-limited catchments (Figure 3). This may be because P is frequent and significant enough to exceed water demands, allowing S to fill up (e.g., wet water year in Luquillo, Figure 3). In water-limited catchments (e.g., Tilden), we observed that during normal water years, no plateau is accomplished. However, a plateau stage can occur during wet water years (Figure 3). This suggests that the plateau stage is driven by P magnitudes, where individual catchments likely have a S threshold that must be reached to hit the plateau stage. Several researchers have studied event-based precipitation-runoff analyses, explaining that S thresholds (or some proxy thereof, e.g., antecedent precipitation indices) need to be exceeded to generate runoff (McDonnell et al., 2021; Tromp-van Meerveld & McDonnell, 2006). The P, Q and S dynamics observed during the plateau confirm this previous knowledge for systems near the threshold that transition between water- and energy-limited during dry and wet water years, respectively.

4.2.3 | Dry-down

With the onset of the growing season and an increase in ET demand, we transition from the plateau to the dry-down stage of catchment S (Figure 6). During this time, S decreases as Q and ET continuously remove water from the system, faster than incoming P (Figure 4). These observations are supported by others; (Meerveld et al., 2015) observed low S and stream responses in periods of high ET for a catchment in the subtropical southeastern US. In a continental-scale study across the contiguous US and Puerto Rico, (Rossi et al., 2016) described how high ET could lower the soil moisture before P occurs, decreasing the relative role of antecedent S on runoff generation. While we see the dry-down stage in watersheds across the water-to-energy limitation gradient (Figure 3), we anticipate that different hydrologic budget components drive S dynamics during this stage in different hydroclimates. In energy-limited landscapes, the dry-down stage is likely controlled by seasonality in ET (Gnann et al., 2020; Maeda et al., 2017), as these systems are often recognized to have limited seasonality in P (i.e., P continues to occur throughout the growing season). However, in water-limited landscapes, the dry-down is likely controlled by seasonality in both P and ET (Cramer & Hoffman, 2015; Feng et al., 2019). For example, in catchments with Mediterranean climates, such as Tilden, the water balance during the dry-down is dominated by ET and Q, as P events are uncommon during this stage. The asynchrony between P and ET (Feng et al., 2019) in these types of landscapes leads to a more marked dry-down stage, which differs from the above-described controlling mechanisms for energy-limited landscapes. The dry-down stage ends once the system transitions into the wet up stage.

This conceptual framework for categorizing S behaviour in catchments is consistent with other studies. For example, Fovet et al. (2015) used hysteresis analysis of daily S and Q in a maritime watershed in northwest France and described four distinctive periods in which the S-Q relationship highlighted different hydrologic processes. First, they noticed that P was partitioned towards S at the end of the

dry periods. Second, Fovet et al. (2015) observed a wetting period, which resulted in S saturation in the riparian aquifer, allowing for more S supply to Q while hillslope S continued to be filled. This was followed by a period in which hillslope S was filled and started contributing to Q. Lastly, they described a period in which P declined, riparian S decreased and Q was sustained by hillslope S. Interestingly, Fovet et al. (2015) did not consider the role of ET in their characterization of the different periods. The S-Q relationship presented by (Fovet et al., 2015) was also proposed by Spence et al. (2010) for a large watershed in the Canadian shield. Both studies showed the critical role of S for runoff generation and highlighted the importance of intra-annual variability, which we found when disaggregating the hysteresis pattern by the S stages (Figure 5). The conceptual model of storage stages in the present study thus advances ideas proposed by Fovet et al. (2015) and Spence et al. (2010) by applying them across the water/energy gradient.

4.3 | Seasonal precipitation partitioning controls hysteretic behaviour of runoff

This study documents relatively higher RR in the wet-up than in the dry-down stage for a given S value for the threshold catchments (Tilden, Calhoun; Figure 5). This essential distinguishing characteristic of the S and RR relationship illustrates the complexity of S variability at threshold catchments that we did not observe in the two energy-limited systems studied here (Figure 5). For the two systems at the threshold of water$-$/energy-limitation, the same S amount was partitioned to ET or Q differently throughout the year, depending on the S stage (Figure 5), which directly impacted how much water contributed to the stream (i.e., the RR).

Two different catchment storage reservoirs, direct and indirect storage, have been described to explain the dynamic behaviours in the S-Q relationships of watersheds (Dralle et al., 2018), which can result in the hysteretic behaviour of these two components of the water balance. Direct storage is hydraulically connected to the stream, and it explains the direct relationship between S and Q (i.e., Q is explicitly sensitive to variations of direct storage). In a saturated porous media, direct storage is the amount of water stored above field capacity. On the other hand, indirect storage is not hydraulically connected to the stream, and equals the amount of water stored below field capacity. Thus, indirect storage can change in amount without directly affecting Q (Dralle et al., 2018). The wet-up and dry-down S stages highlight the transition between two extremes of catchment storage. We can see the predominant influence of indirect storage in a landscape at the beginning of the wet-up (or at the end of the dry-down), while complete saturation at the maximum direct storage could dominate during the plateau. Further, the difference in RR during the wet-up and dry-down could be a reflection of the redistribution of water between direct and indirect storages as a consequence of plant uptake during the growing season. The lack of hysteresis in the two more energy-limited catchments for the water years analysed is likely due to the lower S variability observed (i.e., S stays 'full' in

these two catchments) probably, because P is largely partitioned to direct storage in these much wetter catchments.

The present study does not address the role of ET in the redistribution of water into different S reservoirs during the dry-down directly, but we suspect that ET magnitude may influence whether P gets distributed into indirect or direct storage. This, in turn, may help explain the hysteretic behaviour of the SS-RR relationships observed at Tilden and Calhoun. We hypothesize redistribution of the incoming P during the dry-down stage into less hydraulically active but more plant-accessible storage zones (Dralle et al., 2018). This is consistent with the findings of ecohydrological studies of recent years that highlight how vegetation can tap into storage pools without affecting streamflow (Chang et al., 2019; Evaristo & McDonnell, 2017; Nehemy et al., 2021; Sprenger et al., 2016). Moreover, it has been documented in the literature that plants can remove significant water volumes stored in saprolite and rock moisture (Hahm et al., 2019; McCormick et al., 2021; Rempe & Dietrich, 2018) which are commonly underappreciated parts of catchment storage, and that do not necessarily contribute directly to Q.

Even though the ecohydrology community has continued to improve collective knowledge on vegetation water use (Dawson & Ehleringer, 1991; Li et al., 2019; McLaughlin et al., 2017; Meißner et al., 2014; Oerter et al., 2019; Penna et al., 2018), the mechanisms that explain where vegetation access water are poorly known. For example, (Volkmann et al., 2016) showed that different vegetation types growing in the same area used water from different depths. Similarly, (Allen et al., 2019) showed that plant species in the same environment favoured the use of water with different seasonal origins. With our analysis, we cannot assess the mechanisms by which plants access water in the watersheds studied. However, by showing the disparate P partitioning during the dry-down stage relative to the wet-up stage of catchment storage, the relatively simple analysis of the water balance in the present study highlights the necessity for understanding ET (especially transpiration) when modelling the terrestrial water budget (Jasechko et al., 2013; Schlesinger & Jasechko, 2014).

The replenishment of these vegetation-preferred storage pools is relatively unexplored. How these stores receive inflow during the wet-up stage may help to explain S-RR hysteresis (Figure 5), which highlights the effects of intra-annual S variations for runoff generation in catchments at the threshold. Using storage stages as a framework to separate periods of the water year with distinct hydrologic partitioning characteristics, we may be able to further enhance our understanding of the relative importance of ET as a controlling parameter in S-RR relationships in watersheds.

4.4 | Limitations and future considerations

The work discussed here was restricted to two water years at each site, which introduces limitations in generalizing our findings. Specifically, data availability restricted our work for our two main study watersheds (Calhoun and Tilden); monitoring at the sites occurred

during a short duration, which included a wet and a normal water year. Thus, while lower Hafren and Luquillo have longer datasets, we selected water years with similar P percentiles. The analysis used in this study can be improved by extending hydrologic observations to include a greater range of hydrologic conditions., for example, pairs of water years with similar total P, but different antecedent conditions. While our data availability did not allow for such an analysis, we recognize potential future research avenues in testing our discussion with longer time series.

Measurements in all the water balance parameters contain some degree of uncertainty/error. In Particular, catchment ET measurements are highly uncertain. However, it is worth noting that our analysis does not depend on the magnitude of daily ET. Our conceptual model is based on the temporal variability of the water balance parameters within a water year. Notably, the stages of catchment storage can be identified by the shape of the storage curve (Figure 2). Thus, uncertainties in the magnitude of ET, as long as the errors are uniformly distributed, should result in similar S shapes but shifted in magnitude.

5 | IMPLICATIONS AND CONCLUSION

This study elucidates the intra-annual variability in runoff generation in response to changes in S in watersheds that exist over a range of hydroclimatic conditions. Our analysis sought to improve our conceptual understanding of the diversity of catchment behaviour within long-term annual water balance classifications. We observed a characteristic shape in daily storage across water years in watersheds at the water−/energy-limitation threshold, where systems experienced distinct runoff response across wet-up, plateau, and dry-down S stages.

The similarity in intra-annual S variability between the two threshold catchments, notwithstanding their different hydroclimatic zones and long-term positions on opposite sides of the threshold, suggests a characteristic behaviour of catchments close to this threshold. This similitude indicates that for catchments such as Calhoun and Tilden, significant intra-annual changes in S induce marked shifts in runoff generation behaviour that are characteristic of both humid and arid catchments (i.e., intra-annual switch between water- and energy-limited).

The semi-arid watershed (Tilden) shifted between energy-limited and water-limited for the wet and normal water years. This variability led to differences in the degree or presence of S stages that occurred during each individual water year. In a normal water year, Tilden displayed only a wet-up and dry-down stage, as water demands were insufficient to achieve the plateau. However, this catchment displayed the three S stages during the wet water year. In the humid Calhoun, we observed the three S stages for both water years, highlighting this system's position at the threshold of water−/energy-limited hydroclimates, where storage is depleted and recharged each water year. However, separating the annual hydroclimatic conditions by events (and monthly) at Calhoun showcased how this system switches from water-limited to energy-limited within the year, which is otherwise masked in aggregated annual averages (Figure 3).

Our analysis shows that catchment behaviour is not 100% uniform throughout a water year. However, it is worth noticing that the classification of catchments as either water-limited or energy-limited is not a binary classification. When we classify a catchment as water-limited, it does not necessarily mean that it displays a water-limited behaviour the entirely of the time, but rather that it behaves as a water-limited system most of the time (Creed et al., 2014). For example, as discussed earlier, Calhoun switches between water-limited and energy-limited at the event scale, but overall, in terms of the number of events, it is predominantly energy-limited. Thus, the events that occur during the wet-up and the dry-down, which are associated with water-limitation, could be considered outliers. On the other hand, Tilden, or any other catchment around the globe that is labelled as water-limited based on annual data, may also switch back and forth at the event scale, but overall it is predominantly water-limited (i.e., most of the events occur during the wet-up and the dry down). The question then becomes: what is the importance of these outlier events in understanding the overall function or hydrologic importance of these watersheds?

The outlier events that describe the variability in behaviour between water/energy-limitation for catchments at the threshold are important for process understanding, especially for runoff generation during shoulder seasons. We found that the wet-up and the dry-down correspond to the transition periods between wet and dry seasons. The 'outlier' events matter because they can be associated with very high precipitation intensities and volumes (e.g., atmospheric river events, hurricanes). This phenomenon is expected to become more evident with climate change. In California (Tilden), fewer but more intense precipitation events are expected to occur during the shoulder seasons (Swain et al., 2018). Similarly, there is an increase in the number and magnitude of hurricanes in the southeastern US (Calhoun) (Wang et al., 2011). In other words, many of the changes in hydroclimatic forces anticipated due to climate change will occur at the time when the 'outlier' events are already occurring. Thus, outlier events are likely to become less outlying.

Further, our findings are important for water resources management. Here, we showed that precipitation events that occur during the wet-up and the dry-down display characteristics common to water-limited systems, whereas precipitation events that occur in the plateau display characteristics common to energy-limited systems. As human population and thus water demand grows, we have started to manage storm flows through practices such as managed aquifer recharge, where we engineer catch basins to purposefully infiltrate stormflow to manually recharge the subsurface (Levintal et al., 2022; Ma et al., 2022). In water-limited systems, the standard practice is to remove water in times of surplus (Dahlke et al., 2018). The framework presented here can help us identify periods of surplus (e.g., plateau stage). On the other hand, in energy-limited systems, where precipitation is relatively uniform, we usually do not think about hydroclimate seasonality, often focusing more heavily on routing water off of the landscape efficiently. These predominant management strategies have an implicit assumption of hydroclimatic stationarity embedded within them. We believe our work can serve as a first assessment for periods

in which managed aquifer recharge should not be performed in these systems (e.g., in the wet-up and dry-down stages of catchment storage). During these periods, the stream discharge might not be sufficient to sustain other environmental and ecological needs, such as water for fish and amphibians that dwell in streams. Similarly, these storage states may provide conceptual tools for determining when to incorporate strategies akin to managed aquifer recharge in regions where it has not traditionally been used. For example, encouraging retention of water in upland aquifers that feed reservoirs in humid, energy-limited regions.

In conclusion, categorizing watersheds as energy- or water-limited based on long-term annual water balances has been a fundamental approach for explaining variability in runoff generation across landscapes with various hydroclimatic conditions. However, annual water balance studies may 'miss' the intra-annual variability in runoff generation, which may obscure the differences and similarities between water- and energy-limited catchments, especially in landscapes with long-term hydrology that places them close to the threshold between water- and energy-limitation. We present a framework for comparing S-RR at intra-annual scales in catchments across the hydroclimatic spectrum that display different S stages across the water year. Our S stage framework can be used as a unifying concept to make more robust cross-catchment comparisons that include the non-stationarity of hydroclimates. Improving our knowledge of the P partitioning in catchments at the threshold of water−/energy-limited hydroclimates might arise from explaining these catchments' water balance components and multi-scale hydrologic controls (e.g., S, RR) rather than using the Budyko space.

DATA AVAILABILITY STATEMENT

The data that support the findings of this study are available from the corresponding author upon reasonable request.

ORCID

Emilio Grande https://orcid.org/0000-0003-3995-0380
Margaret A. Zimmer https://orcid.org/0000-0001-8287-1923
John M. Mallard https://orcid.org/0000-0002-0494-9024

REFERENCES

Allen, R., Pereira, L., Raes, D., & Smith, M. (1998). *Crop evapotranspiration-guidelines for computing crop water requirements*. FAO.

Allen, S. T., Kirchner, J. W., Braun, S., Siegwolf, R. T. W., & Goldsmith, G. R. (2019). Seasonal origins of soil water used by trees. *Hydrology and Earth System Sciences*, 23(2), 1199–1210. https://doi.org/10.5194/hess-23-1199-2019

Aulenbach, B. T., & Peters, N. E. (2018). Quantifying climate-related interactions in shallow and deep storage and evapotranspiration in a forested, seasonally water-limited watershed in the southeastern United States. *Water Resources Research*, 54(4), 3037–3061. https://doi.org/10.1002/2017WR020964

Blume, T., Zehe, E., & Bronstert, A. (2007). Rainfall—Runoff response, event-based runoff coefficients and hydrograph separation. *Hydrological Sciences Journal*, 52(5), 843–862. https://doi.org/10.1623/hysj.52.5.843

Budyko, M. I. (1974). *Climate and life*. Academic Press.

Buss, H. L., Brantley, S. L., Scatena, F. N., Bazilievskaya, E. A., Blum, A., Schulz, M., Jiménez, R., White, A. F., Rother, G., & Cole, D. (2013). Probing the deep critical zone beneath the Luquillo experimental Forest, Puerto Rico. *Earth Surface Processes and Landforms*, 38(10), 1170–1186. https://doi.org/10.1002/esp.3409

California Actual Evapotranspiration (CalETa) Mapping Program. California Data Exchange Center - Query Tools. https://cdec.water.ca.gov/ 2019.

Camporese, M., Paniconi, C., Putti, M., & McDonnell, J. J. (2019). Fill and spill hillslope runoff representation with a Richards equation-based model. *Water Resources Research*, 55(11), 8445–8462. https://doi.org/10.1029/2019WR025726

Chang, E., Li, P., Li, Z., Xiao, L., Zhao, B., Su, Y., & Feng, Z. (2019). Using water isotopes to analyze water uptake during vegetation succession on abandoned cropland on the loess plateau, China. *CATENA*, 181, 104095. https://doi.org/10.1016/j.catena.2019.104095

Choi, J.-R., Kim, B.-S., Kang, D.-H., & Chung, I.-M. (2022). Evaluation of water supply capacity of a small Forested Basin water supply facilities using SWAT model and flow recession curve. *KSCE Journal of Civil Engineering*, 26, 3665–3675. https://doi.org/10.1007/s12205-022-1075-4

Contra Costa Soil Survey. 1981. *Soil Survey for Contra Costa County, California. United States Department of Agriculture*. Soil Conservation Service. (pp. 122).

Cramer, M. D., & Hoffman, M. T. (2015). The consequences of precipitation seasonality for mediterranean-ecosystem vegetation of South Africa. *PLoS One*, 10(12), e0144512. https://doi.org/10.1371/journal.pone.0144512

Creed, I. F., Spargo, A. T., Jones, J. A., Buttle, J. M., Adams, M. B., Beall, F. D., Booth, E. G., Campbell, J. L., Clow, D., Elder, K., Green, M. B., Grimm, N. B., Miniat, C., Ramlal, P., Saha, A., Sebestyen, S., Spittlehouse, D., Sterling, S., Williams, M. W., ... Yao, H. (2014). Changing forest water yields in response to climate warming: Results from long-term experimental watershed sites across North America. *Global Change Biology*, 20(10), 3191–3208. https://doi.org/10.1111/gcb.12615

Dahlke, H. E., LaHue, G. T., Mautner, M. R. L., Murphy, N. P., Patterson, N. K., Waterhouse, H., Yang, F., & Foglia, L. (2018). Chapter eight - managed aquifer recharge as a tool to enhance sustainable groundwater management in California: Examples from field and modeling studies. In J. Friesen & L. Rodríguez-Sinobas (Eds.), *Advances in chemical pollution, environmental management and protection* (pp. 215–275). Elsevier. https://doi.org/10.1016/bs.apmp.2018.07.003

Davies, J. A. C., & Beven, K. (2015). Hysteresis and scale in catchment storage, flow and transport. *Hydrological Processes*, 29(16), 3604–3615. https://doi.org/10.1002/hyp.10511

Dawson, T. E., & Ehleringer, J. R. (1991). Streamside trees that do not use stream water. *Nature*, 350(6316), 335–337. https://doi.org/10.1038/350335a0

Detty, J. M., & McGuire, K. J. (2010). Topographic controls on shallow groundwater dynamics: Implications of hydrologic connectivity between hillslopes and riparian zones in a till mantled catchment. *Hydrological Processes*, 24(16), 2222–2236. https://doi.org/10.1002/hyp.7656

Dralle, D. N., Hahm, W. J., Rempe, D. M., Karst, N. J., Thompson, S. E., & Dietrich, W. E. (2018). Quantification of the seasonal hillslope water storage that does not drive streamflow: Catchment storage that does not drive streamflow. *Hydrological Processes*, 32(13), 1978–1992. https://doi.org/10.1002/hyp.11627

Evaristo, J., & McDonnell, J. J. (2017). Prevalence and magnitude of groundwater use by vegetation: A global stable isotope meta-analysis. *Scientific Reports*, 7(1), 44110. https://doi.org/10.1038/srep44110

Evers, S. M., Knight, T. M., Inouye, D. W., Miller, T. E. X., Salguero-Gómez, R., Iler, A. M., & Compagnoni, A. (2021). Lagged and dormant season climate better predict plant vital rates than climate during the growing season. *Global Change Biology*, 27(9), 1927–1941. https://doi.org/10.1111/gcb.15519

Feng, X., Thompson, S. E., Woods, R., & Porporato, A. (2019). Quantifying asynchronicity of precipitation and potential evapotranspiration in mediterranean climates. *Geophysical Research Letters*, 46(24), 14692–14701. https://doi.org/10.1029/2019GL085653

Fovet, O., Ruiz, L., Hrachowitz, M., Faucheux, M., & Gascuel-Odoux, C. (2015). Hydrological hysteresis and its value for assessing process consistency in catchment conceptual models. *Hydrology and Earth System Sciences*, 19(1), 105–123. https://doi.org/10.5194/hess-19-105-2015

Fuka D, Walter M, Archibald D, Steenhuis T, Easton Z. 2018. EcoHydRology.

Garcia, E. S., & Tague, C. L. (2015). Soil storage influences climate–evapotranspiration interactions in three western United States catchments. *Hydrology and Earth System Sciences Discussions*, 12(8), 7893–7931. https://doi.org/10.5194/hessd-12-7893-2015

Gnann, S. J., Howden, N. J. K., & Woods, R. A. (2020). Hydrological signatures describing the translation of climate seasonality into streamflow seasonality. *Hydrology and Earth System Sciences*, 24(2), 561–580. https://doi.org/10.5194/hess-24-561-2020

Grande, E., Visser, A., Beitz, P., & Moran, J. (2019). Examination of nutrient sources and transport in a catchment with an Audubon certified golf course. *Water*, 11(9), 1923. https://doi.org/10.3390/w11091923

Grande, E., Visser, A., & Moran, J. E. (2020). Catchment storage and residence time in a periodically irrigated watershed. *Hydrological Processes*, 34(14), 1–17. https://doi.org/10.1002/hyp.13798

Graymer RW. 2000. Geologic map and map database of the Oakland metropolitan area, Alameda, Contra Costa, and San Francisco Counties, California.

Hahm, W. J., Rempe, D. M., Dralle, D. N., Dawson, T. E., Lovill, S. M., Bryk, A. B., Bish, D. L., Schieber, J., & Dietrich, W. E. (2019). Lithologically controlled subsurface critical zone thickness and water storage capacity determine regional plant community composition. *Water Resources Research*, 55(4), 3028–3055. https://doi.org/10.1029/2018WR023760

Hailegeorgis, T. T., Alfredsen, K., Abdella, Y. S., & Kolberg, S. (2016). Evaluation of storage–discharge relationships and recession analysis-based distributed hourly runoff simulation in large-scale, mountainous and snow-influenced catchment. *Hydrological Sciences Journal*, 61(16), 2872–2886. https://doi.org/10.1080/02626667.2016.1170939

Harman, C. J. (2015). Time-variable transit time distributions and transport: Theory and application to storage-dependent transport of chloride in a watershed. *Water Resources Research*, 51(1), 1–30. https://doi.org/10.1002/2014WR015707

Hay, C. H., & Irmak, S. (2009). Actual and reference evaporative losses and surface coefficients of a maize field during nongrowing (dormant) periods. *Journal of Irrigation and Drainage Engineering*, 135(3), 313–322. https://doi.org/10.1061/(ASCE)IR.1943-4774.0000001

Hewlett, J. D., & Hibbert, A. R. (1967). Factors affecting the response of small watersheds to precipitation in humid areas. *Forest Hydrology*, 33, 275–290.

Jasechko, S., Sharp, Z. D., Gibson, J. J., Birks, S. J., Yi, Y., & Fawcett, P. J. (2013). Terrestrial water fluxes dominated by transpiration. *Nature*, 496(7445), 347–350. https://doi.org/10.1038/nature11983

Jones, J. A., Creed, I. F., Hatcher, K. L., Warren, R. J., Adams, M. B., Benson, M. H., Boose, E., Brown, W. A., Campbell, J. L., Covich, A., Clow, D. W., Dahm, C. N., Elder, K., Ford, C. R., Grimm, N. B., Henshaw, D. L., Larson, K. L., Miles, E. S., Miles, K. M., … Williams, M. W. (2012). Ecosystem processes and human influences regulate streamflow response to climate change at long-term ecological research sites. *Bioscience*, 62(4), 390–404. https://doi.org/10.1525/bio.2012.62.4.10

Kirchner, J. W. (2009). Catchments as simple dynamical systems: Catchment characterization, rainfall-runoff modeling, and doing hydrology backward. *Water Resources Research*, 45(2), 1–34. https://doi.org/10.1029/2008WR006912

Kottegoda, N. T., Natale, L., & Raiteri, E. (2000). Daily streamflow simulation using recession characteristics. *Journal of Hydrologic Engineering*, 5(1), 17–24. https://doi.org/10.1061/(ASCE)1084-0699(2000)5:1(17)

Lapides, D. A., Hahm, W. J., Rempe, D. M., Dietrich, W. E., & Dralle, D. N. (2022). Controls on stream water age in a saturation overland flow-dominated catchment. *Water Resources Research*, 58(4), e2021WR031665. https://doi.org/10.1029/2021WR031665

Levintal, E., Kniffin, M. L., Ganot, Y., Marwaha, N., Murphy, N. P., & Dahlke, H. E. (2022). Agricultural managed aquifer recharge (ag-MAR)—A method for sustainable groundwater management: A review. *Critical Reviews in Environmental Science and Technology*, 1–24. https://doi.org/10.1080/10643389.2022.2050160

Li, H., Si, B., Wu, P., & McDonnell, J. J. (2019). Water mining from the deep critical zone by apple trees growing on loess. *Hydrological Processes*, 33(2), 320–327. https://doi.org/10.1002/hyp.13346

Ma, X., Dahlke, H., Duncan, R., Doll, D., Martinez, P., Lampinen, B., & Volder, A. (2022). Winter flooding recharges groundwater in almond orchards with limited effects on root dynamics and yield. *California Agriculture*, 76(2), 1–7.

Maeda, E. E., Ma, X., Wagner, F. H., Kim, H., Oki, T., Eamus, D., & Huete, A. (2017). Evapotranspiration seasonality across the Amazon Basin. *Earth System Dynamics*, 8(2), 439–454. https://doi.org/10.5194/esd-8-439-2017

Mallard J. 2020. Hydrologic functioning of low-relief, deep soil watersheds and hydrologic legacies of intensive agriculture in the Calhoun critical zone observatory, South Carolina, USA. Doctor od Philosophy, Duke University, North Carolina, USA. https://dukespace.lib.duke.edu/dspace/bitstream/handle/10161/20983/Mallard_duke_0066D_15696.pdf?sequence=1.

McCarter, C. P. R., Sebestyen, S. D., Eggert, S. L., Kolka, R. K., & Mitchell, C. P. J. (2020). Changes in hillslope hydrology in a perched, shallow soil system due to clearcutting and residual biomass removal. *Hydrological Processes*, 34(26), 5354–5369. https://doi.org/10.1002/hyp.13948

McCormick, E. L., Dralle, D. N., Hahm, W. J., Tune, A. K., Schmidt, L. M., Chadwick, K. D., & Rempe, D. M. (2021). Widespread woody plant use of water stored in bedrock. *Nature*, 597(7875), 225–229. https://doi.org/10.1038/s41586-021-03761-3

McDonnell, J. J., Spence, C., Karran, D. J., van Meerveld, H. J., & Harman, C. J. (2021). Fill-and-spill: A process description of runoff generation at the scale of the beholder. *Water Resources Research*, 57(5), e2020WR027514. https://doi.org/10.1029/2020WR027514

McGlynn, B. L., & McDonnell, J. J. (2003a). Role of discrete landscape units in controlling catchment dissolved organic carbon dynamics. *Water Resources Research*, 39(4), 1–18. https://doi.org/10.1029/2002WR001525

McGlynn, B. L., & McDonnell, J. J. (2003b). Quantifying the relative contributions of riparian and hillslope zones to catchment runoff: Small catchment runoff sources. *Water Resources Research*, *39*(11), 1–20. https://doi.org/10.1029/2003WR002091

McLaughlin, B. C., Ackerly, D. D., Klos, P. Z., Natali, J., Dawson, T. E., & Thompson, S. E. (2017). Hydrologic refugia, plants, and climate change. *Global Change Biology*, *23*(8), 2941–2961. https://doi.org/10.1111/gcb.13629

Meerveld, H. J., Seibert, J., & Peters, N. E. (2015). Hillslope–riparian-stream connectivity and flow directions at the Panola Mountain research watershed. *Hydrological Processes*, *29*(16), 3556–3574. https://doi.org/10.1002/hyp.10508

Meißner, M., Köhler, M., Schwendenmann, L., Hölscher, D., & Dyckmans, J. (2014). Soil water uptake by trees using water stable isotopes (δ2H and δ18O)—a method test regarding soil moisture, texture and carbonate. *Plant and Soil*, *376*(1–2), 327–335. https://doi.org/10.1007/s11104-013-1970-z

Merz, R., Blöschl, G., & Parajka, J. (2006). Spatio-temporal variability of event runoff coefficients. *Journal of Hydrology*, *331*(3–4), 591–604. https://doi.org/10.1016/j.jhydrol.2006.06.008

Nehemy, M. F., Benettin, P., Asadollahi, M., Pratt, D., Rinaldo, A., & McDonnell, J. J. (2021). Tree water deficit and dynamic source water partitioning. *Hydrological Processes*, *35*(1), e14004. https://doi.org/10.1002/hyp.14004

Nippgen, F., McGlynn, B. L., Emanuel, R. E., & Vose, J. M. (2016). Watershed memory at the coweeta hydrologic laboratory: The effect of past precipitation and storage on hydrologic response: Watershed memory at the coweeta hydrologic laboratory. *Water Resources Research*, *52*(3), 1673–1695. https://doi.org/10.1002/2015WR018196

NOAA. 2015. National centers for environmental information, state of the climate: Hurricanes and tropical storms for september 2015 https://www.ncdc.noaa.gov/sotc/tropical-cyclones/201509.

Oerter, E. J., Siebert, G., Bowling, D. R., & Bowen, G. (2019). Soil water vapour isotopes identify missing water source for streamside trees. *Ecohydrology*, *12*(4), e2083. https://doi.org/10.1002/eco.2083

Paul G, Townsend P, Schmid B, Chong C, Roberson M, Hawkins T, Smith A, Williams D, Kellar C. 2017. California actual evapotranspiration program http://www.cwemf.org/AMPresentations/2017/s8/3.George_Paul.pdf.

Peel, M. C., Finlayson, B. L., & McMahon, T. A. (2007). Updated world map of the Köppen-Geiger climate classification. *Hydrology and Earth System Sciences*, *11*(5), 1633–1644. https://doi.org/10.5194/hess-11-1633-2007

Penna, D., Hopp, L., Scandellari, F., Allen, S. T., Benettin, P., Beyer, M., Geris, J., Klaus, J., Marshall, J. D., Schwendenmann, L., Volkmann, T. H. M., Freyberg, J., Amin, A., Ceperley, N., Engel, M., Frentess, J., Giambastiani, Y., McDonnell, J., Zuecco, G., … Kirchner, J. (2018). Ideas and perspectives: Tracing terrestrial ecosystem water fluxes using hydrogen and oxygen stable isotopes - challenges and opportunities from an interdisciplinary perspective. *Biogeosciences*, *15*(21), 6399–6415. https://doi.org/10.5194/bg-15-6399-2018

Reaver, N. G. F., Kaplan, D. A., Klammler, H., & Jawitz, J. W. (2022). Theoretical and empirical evidence against the Budyko catchment trajectory conjecture. *Hydrology and Earth System Sciences*, *26*(5), 1507–1525. https://doi.org/10.5194/hess-26-1507-2022

Rempe, D. M., & Dietrich, W. E. (2018). Direct observations of rock moisture, a hidden component of the hydrologic cycle. *Proceedings of the National Academy of Sciences*, *115*(11), 2664–2669. https://doi.org/10.1073/pnas.1800141115

Richter, D. D., Markewitz, D., Heine, P. R., Jin, V., Raikes, J., Tian, K., & Wells, C. G. (2000). Legacies of agriculture and forest regrowth in the nitrogen of old-field soils. *Forest Ecology and Management*, *138*(1), 233–248. https://doi.org/10.1016/S0378-1127(00)00399-6

Rinderer, M., Meerveld, I., Stähli, M., & Seibert, J. (2016). Is groundwater response timing in a pre-alpine catchment controlled more by topography or by rainfall? *Hydrological Processes*, *30*(7), 1036–1051. https://doi.org/10.1002/hyp.10634

Rose, S., & Peters, N. E. (2001). Effects of urbanization on streamflow in the Atlanta area (Georgia, USA): A comparative hydrological approach. *Hydrological Processes*, *15*(8), 1441–1457. https://doi.org/10.1002/hyp.218

Rossi, M. W., Whipple, K. X., & Vivoni, E. R. (2016). Precipitation and evapotranspiration controls on daily runoff variability in the contiguous United States and Puerto Rico. *Journal of Geophysical Research: Earth Surface*, *121*(1), 128–145. https://doi.org/10.1002/2015JF003446

Rouholahnejad Freund, E., & Kirchner, J. W. (2017). A Budyko framework for estimating how spatial heterogeneity and lateral moisture redistribution affect average evapotranspiration rates as seen from the atmosphere. *Hydrology and Earth System Sciences*, *21*(1), 217–233. https://doi.org/10.5194/hess-21-217-2017

Santos, A. C., Portela, M. M., & Schaefli, B. (2018). Application of an analytical model to obtain daily flow duration curves for different hydrological regimes in Switzerland. *International Journal of Environmental and Ecological Engineering*, *12*(11), 694–700.

Schlesinger, W. H., & Jasechko, S. (2014). Transpiration in the global water cycle. *Agricultural and Forest Meteorology*, *189–190*, 115–117. https://doi.org/10.1016/j.agrformet.2014.01.011

Silver, W., & Leon, M. (2019). Precipitation, reservoir height, streamflow/discharge – schoolyard data jam – Puerto Rico – (1990–2016). HydroShare.

Singh, N. K., Emanuel, R. E., Nippgen, F., McGlynn, B. L., & Miniat, C. F. (2018). The relative influence of storm and landscape characteristics on shallow groundwater responses in forested headwater catchments. *Water Resources Research*, *54*(12), 9883–9900. https://doi.org/10.1029/2018WR022681

Smakhtin, V. U. (2001). Low flow hydrology: A review. *Journal of Hydrology*, *240*(3), 147–186. https://doi.org/10.1016/S0022-1694(00)00340-1

Soulsby, C., Birkel, C., Geris, J., Dick, J., Tunaley, C., & Tetzlaff, D. (2015). Stream water age distributions controlled by storage dynamics and nonlinear hydrologic connectivity: Modeling with high-resolution isotope data. *Water Resources Research*, *51*(9), 7759–7776. https://doi.org/10.1002/2015WR017888

Spence, C. (2010). A paradigm shift in hydrology: Storage thresholds across scales influence catchment runoff generation: Paradigm shift in hydrology. *Geography Compass*, *4*(7), 819–833. https://doi.org/10.1111/j.1749-8198.2010.00341.x

Spence, C., Guan, X. J., Phillips, R., Hedstrom, N., Granger, R., & Reid, B. (2010). Storage dynamics and streamflow in a catchment with a variable contributing area. *Hydrological Processes*, *24*(16), 2209–2221. https://doi.org/10.1002/hyp.7492

Sprenger, M., Leistert, H., Gimbel, K., & Weiler, M. (2016). Illuminating hydrological processes at the soil-vegetation-atmosphere interface with water stable isotopes. *Reviews of Geophysics*, *54*(3), 674–704. https://doi.org/10.1002/2015RG000515

Sujono, J., Shikasho, S., & Hiramatsu, K. (2004). A comparison of techniques for hydrograph recession analysis. *Hydrological Processes*, *18*(3), 403–413. https://doi.org/10.1002/hyp.1247

Swain, D. L., Langenbrunner, B., Neelin, J. D., & Hall, A. (2018). Increasing precipitation volatility in twenty-first-century California. *Nature Climate Change*, *8*(5), 427–433. https://doi.org/10.1038/s41558-018-0140-y

Thornthwaite, C. W. (1948). An approach toward a rational classification of climate. *Geographical Review*, *38*(1), 55–94.

Tromp-van Meerveld, H. J., & McDonnell, J. J. (2006). Threshold relations in subsurface stormflow: 2. The fill and spill hypothesis. *Water Resources Research*, *42*(2), 1–11. https://doi.org/10.1029/2004WR003800

van De Giesen, N. C., Stomph, T. J., & de Ridder, N. (2000). Scale effects of Hortonian overland flow and rainfall–runoff dynamics in a west African

catena landscape. *Hydrological Processes*, *14*(1), 165–175. https://doi.org/10.1002/(SICI)1099-1085(200001)14:1<165::AID-HYP920>3.0.CO;2-1

Volkmann, T. H. M., Kühnhammer, K., Herbstritt, B., Gessler, A., & Weiler, M. (2016). A method for in situ monitoring of the isotope composition of tree xylem water using laser spectroscopy. *Plant, Cell & Environment*, *39*(9), 2055–2063. https://doi.org/10.1111/pce.12725

Wagener, T., Sivapalan, M., Troch, P., & Woods, R. (2007). Catchment classification and hydrologic similarity. *Geography Compass*, *1*(4), 901–931. https://doi.org/10.1111/j.1749-8198.2007.00039.x

Wang, Q. J., Pagano, T. C., Zhou, S. L., Hapuarachchi, H. A. P., Zhang, L., & Robertson, D. E. (2011). Monthly versus daily water balance models in simulating monthly runoff. *Journal of Hydrology*, *404*(3), 166–175. https://doi.org/10.1016/j.jhydrol.2011.04.027

Wlostowski, A. N., Molotch, N., Anderson, S. P., Brantley, S. L., Chorover, J., Dralle, D., Kumar, P., Li, L., Lohse, K. A., Mallard, J. M., McIntosh, J. C., Murphy, S. F., Parrish, E., Safeeq, M., Seyfried, M., Shi, Y., & Harman, C. (2021). Signatures of hydrologic function across the critical zone observatory network. *Water Resources Research*, *57*(3), e2019WR026635. https://doi.org/10.1029/2019WR026635

Woolhiser, D. A., Smith, R. E., & Giraldez, J.-V. (1996). Effects of spatial variability of saturated hydraulic conductivity on Hortonian overland flow. *Water Resources Research*, *32*(3), 671–678. https://doi.org/10.1029/95WR03108

Yokoo, Y., Sivapalan, M., & Oki, T. (2008). Investigating the roles of climate seasonality and landscape characteristics on mean annual and monthly water balances. *Journal of Hydrology*, *357*(3), 255–269. https://doi.org/10.1016/j.jhydrol.2008.05.010

Zehe, E., Becker, R., Bárdossy, A., & Plate, E. (2005). Uncertainty of simulated catchment runoff response in the presence of threshold processes: Role of initial soil moisture and precipitation. *Journal of Hydrology*, *315*(1–4), 183–202. https://doi.org/10.1016/j.jhydrol.2005.03.038

Zhou Q, Birkholzer JT, Javandel I, Jordan PD. 2003. Simulation of groundwater flow at the LBNL site using TOUGH2. Proceedings, TOUGH Symposium 2003. Lawrence Berkeley National Laboratory, Berkeley, California, May12-14, 2003: 8.

Zimmerman, J. (2018). Meteorological data from El Verde Field Station: NADP tower ver 1676158. *Environmental Data Initiative*. https://doi.org/10.6073/pasta/d62b391ee1c4e26f918526095a8531ab